Plant sterol biosynthesis: identification of two distinct families of sterol 4α-methyl oxidases

Sylvain DARNET and Alain RAHIER[1]

Centre National de la Recherche Scientifique, Institut de Biologie Moléculaire des Plantes, UPR (Unité Propre de Recherche)-2357, 28 rue Goethe, Strasbourg Cedex 67083, France

In plants, the conversion of cycloartenol into functional phytosterols requires the removal of the two methyl groups at C-4 by an enzymic complex including a sterol 4α-methyl oxidase (SMO). We report the cloning of candidate genes for SMOs in *Arabidopsis thaliana*, belonging to two distinct families termed SMO1 and SMO2 and containing three and two isoforms respectively. SMO1 and SMO2 shared low sequence identity with each other and were orthologous to the *ERG25* gene from *Saccharomyces cerevisiae* which encodes the SMO. The plant SMO amino acid sequences possess all the three histidine-rich motifs (HX_3H, HX_2HH and HX_2HH), characteristic of the small family of membrane-bound non-haem iron oxygenases that are involved in lipid oxidation. To elucidate the precise functions of SMO1 and SMO2 gene families, we have reduced their expression by using a VIGS (virus-induced gene silencing) approach in *Nicotiana benthamiana*. SMO1 and SMO2 cDNA fragments were inserted into a viral vector and *N. benthamiana* inoculated with the viral transcripts. After silencing with SMO1, a substantial accumulation of 4,4-dimethyl-9β,19-cyclopropylsterols (i.e. 24-methylenecycloartanol) was obtained, whereas qualitative and quantitative levels of 4α-methylsterols were not affected. In the case of silencing with SMO2, a large accumulation of 4α-methyl-Δ^7-sterols (i.e. 24-ethylidenelophenol and 24-ethyllophenol) was found, with no change in the levels of 4,4-dimethylsterols. These clear and distinct biochemical phenotypes demonstrate that, in contrast with animals and fungi, in photosynthetic eukaryotes, these two novel families of cDNAs are coding two distinct types of C-4-methylsterol oxidases controlling the level of 4,4-dimethylsterol and 4α-methylsterol precursors respectively.

Key words: *Arabidopsis thaliana*, ERG25, sterol 4α-methyl oxidase, sterol, VIGS (virus-induced gene silencing).

INTRODUCTION

Sterols are ubiquitous and essential membrane components found in all eukaryotes. They regulate membrane fluidity and permeability and interact with lipids and proteins within the membranes [1,2]. They are also precursors of a vast array of bioactive compounds involved in important cellular and developmental processes [3], and plant sterols are particularly linked to brassinosteroid synthesis [4]. The structure of sterols and their biosynthetic pathway differ significantly among fungi, animals and plants [5,6] (Scheme 1). In higher plants, the conversion of cycloartenol (D1; Scheme 2) into functional phytosterols (S1–S3) involves the removal of the two methyl groups at C-4 [5,6]. In animals and fungi, both methyl groups are removed successively early in the biosynthetic pathway [5]. In contrast, in higher plants, although the first C-4-methyl group is removed early from a 4,4-dimethyl-9β,19-cyclopropylsterol precursor, the second C-4-methyl group is eliminated several steps later [5,6] (Scheme 1). The sterol molecule becomes functional as a structural membrane component only after the removal of the two methyl groups at C-4. Thus, in higher plants, the physiological outcome of two biosynthetically distinct C-4-demethylation steps and the role of transient 4,4-dimethylsterol and 4α-methylsterol intermediates with distinct sterol nucleus remain to be elucidated. Recently, *Arabidopsis thaliana* mutants, *hydra* and *fackel*, which are affected in steps before the second C-4-demethylation (Scheme 1), were shown to possess a phenotype distinct from that of classical *dwarf*-like mutants, since they are not rescued with brassinosteroids [7–9]. In these mutants, the accumulation of 4α-methylsterol intermediates, in addition to the modified composition of end-product phytosterols, might be implicated in the severe developmental effects observed. Moreover, mutants of plant deficient in SMO (sterol 4α-methyl oxidase) activity have not been reported so far, possibly reflecting that blockade of the SMO step compromises the viability of plants owing to the accumulation of C-4-methylated sterols. In addition, study of the crucial role of C-4-demethylation in plants is hampered by the lack of inhibitors of the steps involved, as well as by the absence of identification of the committed genes. Thus cloning and precise functional identification of genes involved in plant C-4-demethylation could give important clues for the role of C-4-methylsterols in plants.

Biochemical studies in *Zea mays* have shown that the initial oxidative step of the plant sterol C-4-demethylation process is performed by SMO, which produces a 4α-carboxylic sterol derivative [10]. Subsequently, this acid is oxidatively decarboxylated by 4α-CD (4α-carboxysterol-C-3-dehydrogenase/C-4-decarboxylase) [11] to produce a 3-oxosteroid, which is finally stereospecifically reduced by an NADPH-dependent SR (sterone reductase) [12] to give the corresponding monodemethylated sterol.

Abbreviations used: β-amyrin (Z), olean-12-en-3β-ol; 4α-CD, 4α-carboxysterol-C-3-dehydrogenase/C-4-decarboxylase; CCS, capsanthin-capsorubin synthase; 4,4-dimethylzymosterol (V), 4,4-dimethyl-5α-cholest-8-en-3β-ol; ergosterol, 5α-ergosta-5,7,22-trien-3β-ol; isofucosterol (W), 5α-stigmasta-5,24(24^1)-dien-3β-ol; lanosterol (T), 4,4,14-trimethyl-5α-cholesta-8,24-dien-3β-ol; obtusifoliol (X), 4α,14α-dimethyl-5α-ergosta-8,24(24^1)-dien-3β-ol; RT, reverse transcriptase; SMO, sterol 4α-methyl oxidase; SR, sterone reductase; SUR2, C4-sphingolipid hydroxylase; taraxerol (Y), taraxer-14-en-3β-ol; VIGS, virus-induced gene silencing.

[1] To whom correspondence should be addressed (e-mail enzymo@bota-ulp.u-strasbg.fr).

The nucleotide sequence data reported will appear in DDBJ, EMBL, GenBank® and GSDB Nucleotide Sequence Databases under accession numbers AF039199, AY035393, AY323213, AY078158, AY321103, AY321104, AY163803 and AY163802.

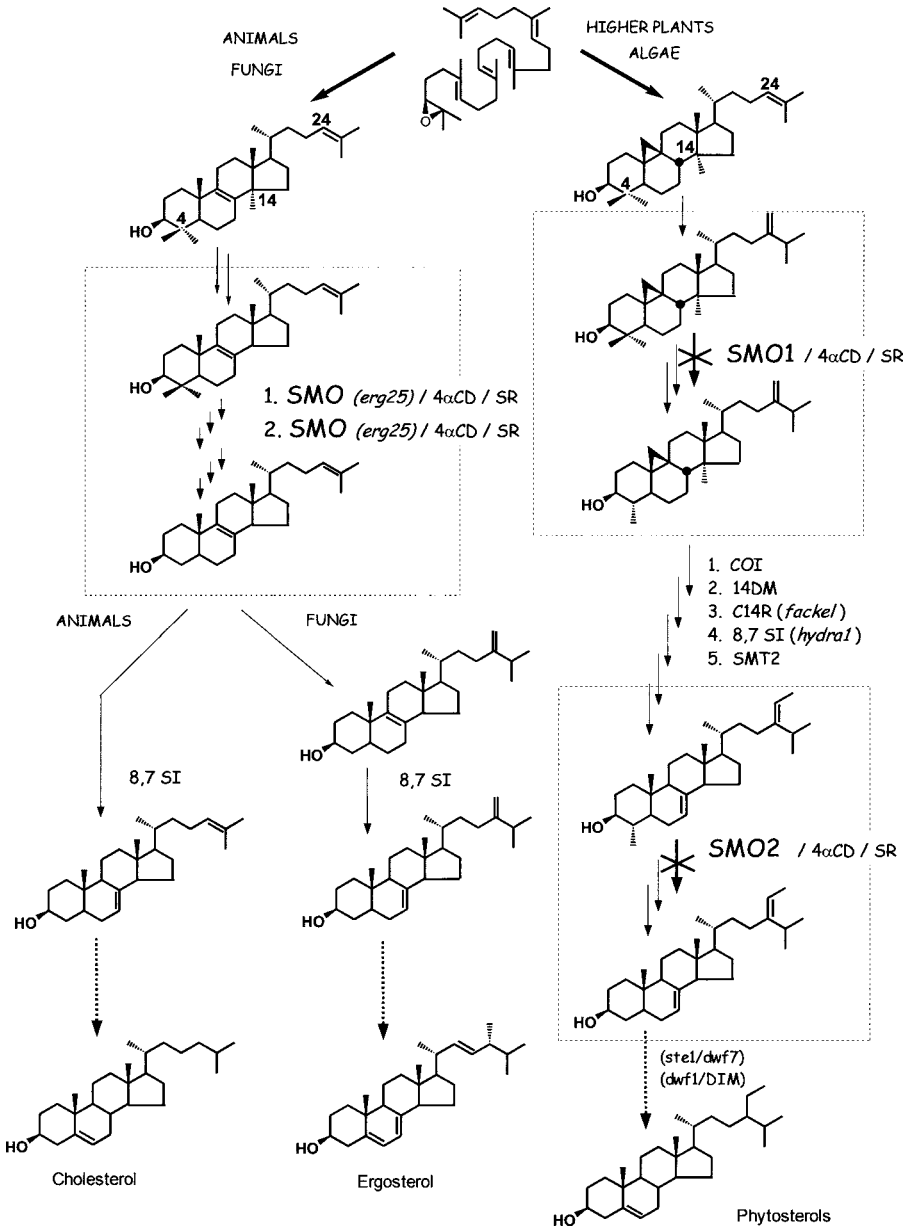

Scheme 1 Simplified sterol biosynthetic pathway in different organisms

Full arrows represent distinct enzymes and arrows with broken lines represent several biosynthetic steps. The boxes represent C-4-demethylation multienzymic complexes, including SMO, 4α-CD and SR. Abbreviations: COI, cycloeucalenol isomerase; 14DM, obtusifoliol 14-demethylase; C14R, $\Delta^{8,14}$-sterol C-14-reductase; 8,7 SI, Δ^{8}-sterol 8,7-isomerase; SMT2, sterol methyltransferase 2.

In the present study, by combining homology and sequence motif searches with knowledge relating to sterol biosynthetic genes across species, candidate genes belonging to two families of plant SMOs (SMO1 and SMO2) have been cloned. To identify the precise functions of these genes, we used a VIGS (virus-induced gene silencing) approach in *Nicotiana benthamiana* with a viral RNA containing cDNA fragments from SMO1 or SMO2. Results indicate clear and distinct biochemical phenotypes, consisting of specific accumulations of substrates of the corresponding SMOs.

MATERIALS AND METHODS

Strains

The *erg25-25c* strain of *Saccharomyces cerevisiae*, deficient in sterol methyl oxidase activity (Mat a *ade5, his3, leu2-3, ura3-52, upc2, erg25-25c*), used in the present study, has been described previously [13].

Plants

N. benthamiana were grown in a greenhouse at 24 °C with a 16 h light/8 h dark cycle.

Plasmids

pVT102U is a yeast shuttle vector, which is optimized for the expression of recombinant proteins in yeast [14]. TTO1A vector is an RNA viral vector described previously [15]. It consists of sequences from tobacco mosaic virus strain U1 (TMV-U1) and tomato mosaic virus (fruit necrosis strain F; ToMV-F).

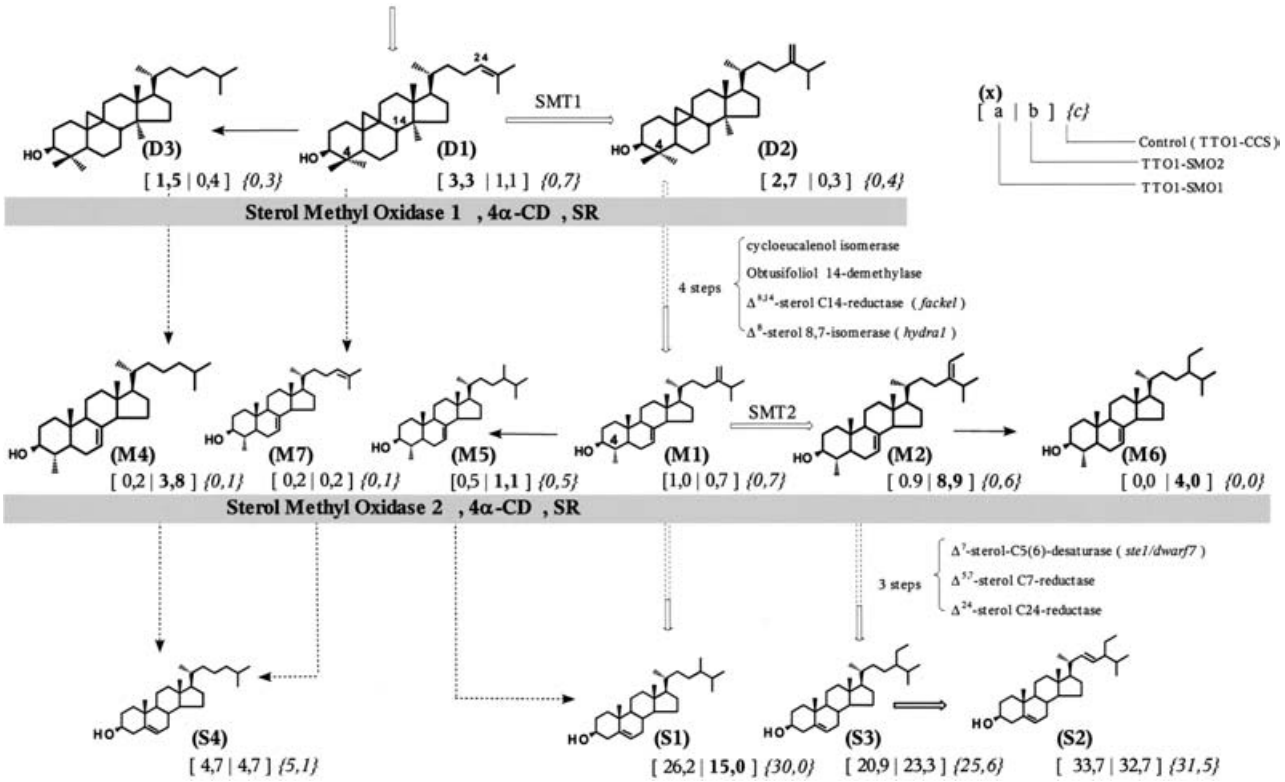

Scheme 2 Accumulation of SMO substrates induced by SMO1 or SMO2 silencing

The major biosynthetic pathway from cycloartenol (D1) to 24-methyl- and 24-ethylsterols is represented by open arrows. Arrows with broken lines represent minor pathways, including several biosynthetic steps. Full arrows indicate pathways revealed after down-regulation of SMO1 or SMO2: D, 4,4-dimethylsterols; M, 4α-methylsterols; S, 4-desmethylsterols. The boxes represent C-4-demethylation multienzymic complexes, including SMO, 4α-CD and SR. Values shown are the content of each compound (% of total sterols) for representative plants infected with TTO1-SMO1, TTO1-SMO2 and TTO1-CCS (control) respectively.

Cloning of SMO1 and SMO2 cDNAs from *Arabidopsis* and *Nicotiana*

Two full-length cDNAs, termed *At*SMO2–1 (*A. thaliana* SMO2-1; GenBank® accession no. AF327853) and *At*SMO2-2 (AF346734) of 783 and 801 bp length respectively, were isolated from *A. thaliana* as described previously [16]. Another family of cDNAs (SMO1) was identified from the *A. thaliana* sequenced genome. It included the full-length *At*SMO1-1 (897 bp, AF039199), which was isolated by screening 350000 recombinants from a cDNA library of developing siliques of *A. thaliana*, ecotype columbia, with the expressed sequence tag clone 182J14T7 (H37509). Two other putative SMO1 cDNAs in the expressed sequence tag and genome *A. thaliana* database were amplified by PCR, namely *At*SMO1-2 (AY035393, 900 bp, full length) with the primers SDR11 (ataatactcgagctaatcgaatttctctcctccattaac), SDF10 (taatatctagaatgatcccatacgcaacaatcgaag) and *At*SMO1-3 (820 bp, AY323213) with the primers SDF16 (ataatatctagaatgatcccttatccaaccgtagaag) and SDR20 (ataatagtcgacgcttcttatggattcgatagcctttat), in a cDNA library of developing siliques. These cDNAs were cloned into the *Xba*I and *Xho*I sites of the pVT102U vector to generate the plasmids pVT-*AtSMO1-1*, pVT-*AtSMO1-2*, pVT-*AtSMO2-1* and pVT-*AtSMO2-2*. Both strands of the insert were sequenced to ensure sequence fidelity.

To amplify SMO cDNAs in *Nicotiana*, primers were designed according to consensus regions of aligned SMO sequences of Solanaceae and the codon usage of *Nicotiana*. Several contigs of cDNA clones from Solanaceae, *Lycopersicon esculatum* and *Solanum tuberosum* were available in the TIGR database: *Le*SMO1 (TC98255), *Le*SMO2 (TC105626), *St*SMO1 (TC72595) and *St*SMO2 (TC32748). To amplify *Nb*SMO (*N. benthamiana* SMO) fragments, PCRs were performed using an aliquot of RT (reverse transcriptase)–PCR obtained from a total RNA extract of stem and degenerated hexamers. A fragment of 732 bp was amplified with the primers SDF42 (ctaataatctgattactatctttactgtc) and SDR34 (ataatatctagaaacatagtgatggtagtcatggtaatc), leading to the partial cDNA termed *Nb*SMO1 (AY321103). A second fragment of 728 bp was amplified with the primers SDF21 (ataatactcgagatggcatccatgattgaatctgcttgg) and SDR45 (cagtccatgtaaacaaatgtcgatg), leading to another partial cDNA termed *Nb*SMO2 (AY321104). Fragments from *N. tabacum* SMOs were cloned from an *N. tabacum* cv BY2 cDNA library. To generate the plasmid TTO1-SMO1, a subfragment of 387 bp of *Nt*SMO1 (AY163803) was cloned in *Avr*II–*Xho*I of TTO1 vector with primers SDF31 (ataatactcgagacaagtttgcccctgccgtc) and SDR34. TTO1-SMO2 was generated by cloning a subfragment of 450 bp of *Nt*SMO2 (AY163802) with primers SDF21/SDR25 (ataatatctagacaagaaaaagaatttcagcagggtgagc).

In vitro transcription, inoculations and analysis of infected plants

Infectious RNA molecules were produced by *in vitro* transcription of the DNA constructs linearized by *Kpn*I, using the SP6 Ribomax transcription kit (Promega, Charbonnières, France). *N. benthamiana* were mechanically inoculated with *in vitro* transcripts as described previously [15]. Virus infection was performed on 5-week-old plants. Plants were analysed 21 days after inoculation.

Quantification of transcript levels in infected *N. benthamiana*

Total RNA from *N. benthamiana* stems were extracted by using the TRIzol® reagent (Invitrogen, Carlsbad, CA, U.S.A.) and treated with DNase to remove any residual DNA. SuperScript II kit (Invitrogen) was used with degenerated hexamers to perform RT–PCRs. We used primers outside the *Nt*SMO fragments inserted into the TTO1 vector, derived from *Nb*cDNAs instead of *Nt*cDNA sequences, to ensure a more specific quantification of endogenous *N. benthamiana* mRNAs.

After optimization, the condition leading to visible bands and unsaturated bands on agarose gels for *Nb*SMO1 was 35 cycles with the oligonucleotides SDF47 (cctaatcttctcttgtgtccctc) and SDR34 to yield a 595 bp product. The same procedure using the oligonucleotides SDF46 (caattgacttgtcttggtgggttt) and SDR50 (caaggactctaagtgagaccc), corresponding to *Nb*SMO2, yielded a 520 bp amplification product. The internal control of RT–PCR quantification was performed using primers for mRNA encoding *N. benthamiana* actin. For *N. tabacum* actin (TOB103; NTU60495) [17], a single-amplification 333 bp product was obtained using the oligonucleotides SDF44 (tattgtgggtcgtcctcgg) and SDR47 (caaggactctaagtaagaccc). All PCR products were sequenced to confirm their identities.

To quantify PCR band intensities, we scanned digital camera images of the gels and assigned to individual bands a relative intensity value by using Jandel Software Sigmagel 1.0. Semi-quantitative RT–PCR was realized by adjusting the number of cycles during the PCR until easily detectable but submaximal amounts of DNA were amplified.

Transformations

S. cerevisiae transformations were performed using the lithium acetate procedure as described previously [18]. Transformed *erg25* yeast strains were selected for uracil prototrophy and grown anaerobically at 30 °C in the presence of exogenous ergosterol (5α-ergosta-5,7,22-trien-3β-ol) and subsequently tested for the ability to grow aerobically without the addition of sterol.

Sterol analysis of *N. benthamiana*

Freeze-dried stems of *N. benthamiana* (100–800 mg) were homogenized with an Ultra-Turrax homogenizer in the presence of methanol/KOH (6 %, w/v) and heated in the same medium at 80 °C under reflux for 3 h. The mixture was diluted with 1 vol. of water and total sterols were extracted three times with 3 vol. of n-hexane. The extract was dried on Na_2SO_4 and evaporated to dryness. Desmethylsterols ($R_f = 0.27$), 4α-methylsterols ($R_f = 0.38$) and 4,4-dimethylsterols ($R_f = 0.44$) were purified by TLC on silica gel 60F254 plates (Merck, Darmstadt, Germany) using one run of ethyl acetate/hexane (3:7, v/v) as a developing solvent. A known amount of cholesterol was added as an internal standard for GC quantification for the 4α-methylsterol and 4,4-dimethylsterol fractions and of coprostane for the desmethylsterol fraction. The 4,4-dimethylsterol fraction was further subjected to an acetylation reaction for one night at room temperature with a mixture of pyridine/acetic anhydride/toluene (1:1:1, by vol., 50 μl) and purified by TLC using one run of ethyl acetate/hexane (3:7) as developing solvent. All three fractions were then analysed by GC using a Varian GC model 8300, which was equipped with a flame ionization detector at 300 °C, a column injector at 250 °C and a fused capillary column [WCOT (silica wall-coated open tubing); internal diameter, 30 m × 0.25 mm] coated with DB1 [(1 % phenyl) methylpolysiloxane; H_2 flow rate, 2 ml/min]. The temperature programme used included a 30 °C/min increase from 60 to 240 °C and then a 2 °C/min increase from 240 to 280 °C. Relative retention time t_R is given with respect to cholesterol ($t_R = 1$). Thorough identification of individual sterols was then performed using a GC-MS spectrometer (Agilent 5973N) equipped with an on-column injector and a capillary column (internal diameter, 30 m × 0.25 mm) coated with DB5 [(5 % phenyl) methylpolysiloxane]. Sterols were unequivocally identified by coincidental retention time and an electron impact spectrum identical with that of authentic standards [19].

Sterol analysis of yeast

Total sterols of yeast were analysed according to the same procedure except that the total extract was analysed by GC, without TLC separation of the different fractions.

RESULTS

Cloning of cDNAs encoding SMOs from *Arabidopsis* and *Nicotiana*

By combining yeast SMO orthologues and sequence motif searches in *A. thaliana*, five SMO cDNAs belonging to two families have been cloned. All *At*SMO amino acid sequences were characterized by the presence of three histidine-rich motifs, namely HX_3H $X_{8\text{ or }9}$ HX_2HH $X_{73\text{ or }75}$ HX_2HH, which exhibit a topology and spacing of amino acids within the histidine motifs typical of the sterol desaturase-like family PFAM01598.

From the multiple alignments of the full-length amino acid sequences of *At*SMOs and sterol-desaturase-like enzymes, we constructed a phylogenetic tree (Figure 1). This tree clearly confirmed the existence of the two families of putative plant SMO isoenzymes SMO1 and SMO2.

Arabidopsis genomic sequences *At4g12110*, *At4g22756*, *At4g22753*, *At1g07420* and *At2g29390*, corresponding to *At*SMO1-1, *At*SMO1-2, *At*SMO1-3, *At*SMO2-1 and *At*SMO2-2 respectively, were used to check manually the intron splicing of these nucleotide sequences using the GTX XAG rule [20] and obtain gene predictions identical with the corresponding cloned cDNAs. The data indicated different gene organizations for *At*SMO1s and *At*SMO2s, i.e. 5 and 7 exons respectively, confirming the occurrence of the two families of genes. Furthermore, we observed that, in addition to the conserved number of exons, the size of exons rarely changes within each family and that the organization of coding domains was conserved and differs between the two families. *At*SMO1 and *At*SMO2 families contain three and two isoforms respectively, and sequence comparisons show that the plant sequences are orthologous to the fungal and mammalian sequences. In addition, cDNA fragments corresponding to each family were isolated in *N. benthamiana*, *Nb*SMO1 (AY321103) and *Nb*SMO2 (AY321104), and in *N. tabacum*, *Nt*SMO1 (AY163803) and *Nt*SMO2 (AY163802).

Expression of the *A. thaliana* cDNAs, *At*SMO1-1, *At*SMO1-2, *At*SMO2-1 and *At*SMO2-2, in the yeast *erg25* strain

These cDNAs were expressed in the *erg25* mutant strain of *S. cerevisiae* lacking the SMO activity, under control of the constitutive alcohol dehydrogenase promoter from the pVT102U (pVT-VOID) shuttle plasmid [14]. In *S. cerevisiae*, the *ERG25* product *Sc*SMO (*S. cerevisiae* SMO) is an essential enzyme, owing to the fact that disruption of *ERG25* is lethal since the *erg25* strain requires ergosterol [or cholesterol (S4)] supplementation for viability [13]. Thus the pVT transformants were first plated on to an ergosterol-containing medium and then replicated on to a medium devoid of sterol. As shown in Figure 2, the *erg25* strain

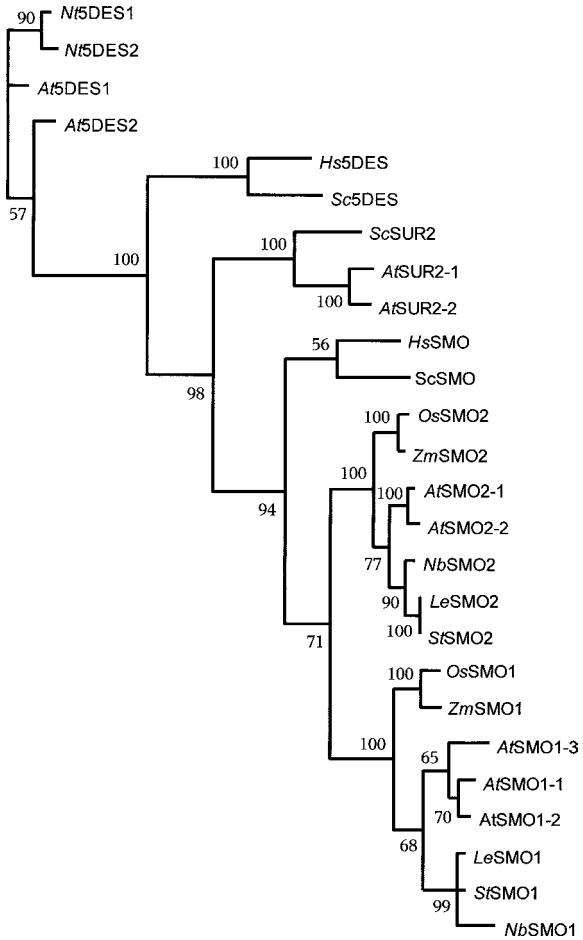

Figure 1 Dendrogram of SMO and sterol-desaturase-like proteins

Amino acid sequences were aligned and used to generate a phylogenetic tree using the program paupsearch based on heuristic methods and distances, coupled with a treeview for visualizing: 5DES, Δ^7-sterol-C-5(6)-desaturase. GenBank® accession numbers are *Sc*5DES: P32353; *At*5DES1: X90454; *At*5DES2: AC021640; *Nt*5DES1: AF081794; *Nt*5DES2: AF099969; *Hs*5DES: 075845; *Sc*SUR2: AAA16608; *At*SUR21: AC013289; *At*SUR22: AC012188; *Os*SMO1: AAK20047; *Zm*SMO1: TC194408; *At*SMO1-3: AY323213; *At*SMO1-1: AF039199; *At*SMO1-2: AY035393; *Le*SMO1: TC98255; *St*SMO1: TC72595; *Nb*SMO1: AY321103; *At*SMO2-1: AF327853; *At*SMO2-2: AF346734; *Nb*SMO2: AY321104; *Le*SMO2: TC105626; *St*SMO2: TC32748; *Os*SMO2: OSJNBb0026k20; *Zm*SMO2: AY078158; *Sc*SMO: P53045; *Hs*SMO: NM006745.

transformed with one among pVT-*ScERG25*, pVT-*AtSMO2-1* and pVT-*AtSMO2-2*, was capable of growing aerobically without ergosterol supplementation, whereas *erg25*-VOID, *erg25*-*At*SMO1-1 and *erg25*-*At*SMO1-2 transformants and *erg25* strains could grow only on an ergosterol-supplemented medium. These results indicate that *At*SMO1-1, *At*SMO1-2 and *Sc*SMO inserts could restore growth, whereas *At*SMO1-1 and *At*SMO1-2 could not restore growth of this strain in the absence of ergosterol (Figure 2).

Next, the sterols of this series of transformants were analysed by GC and GC-MS. Prototrophic strains *erg25*-*Sc*ERG25, *erg25*-*At*SMO2-1 and *erg25*-*At*SMO2-2 accumulated C-4-demethylated sterols including ergosterol in addition to 4,4-dimethylsterols, indicating partial complementation by these *A. thaliana* genes. In contrast, we observed that, similar to *erg25* and *erg25*-VOID, the auxotrophic strains *erg25*-*At*SMO1-1 and *erg25*-*At*SMO1-2 accumulated lanosterol (T) and 4,4-dimethylzymosterol (V), the substrate of the yeast SMO [13,21], but did not accumulate ergosterol (results not shown). Taken together,

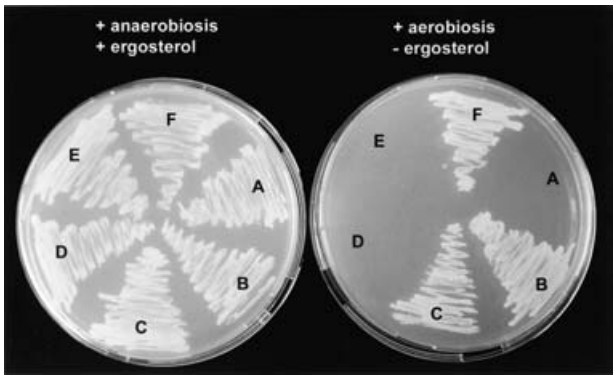

Figure 2 Complementation assays of *erg25-25c* by different plant SMO isoforms

Growth responses of *erg25-25c* transformed with pVT-VOID (A), pVT-*AtSMO21* (B), pVT-*AtSMO2-2* (C), pVT-*AtSMO1-1* (D), pVT-*AtSMO1-2* (E) and pVT-*ScERG25* (F). Transformed *erg-25* was grown aerobically on minimal medium (right panel) or anaerobically on a rich medium, YPG (water solution including 1 % bacto yeast extract, 2 % bacto peptone, 2 % glucose and 2 % bacto agar), supplemented with 2 % (w/v) ergosterol (left panel). All plates were grown for 48 h.

these results clearly indicate that, in contrast with *At*SMO2-1 and *At*SMO2-2, *At*SMO1-1 and *At*SMO1-2 cannot restore endogenous ergosterol synthesis in the *erg25* mutant.

Silencing of endogenous *N. benthamiana* sterol C-4-methyl oxidases

Although mRNAs encoding SMOs from *A. thaliana* are 0.8–0.9 kb long, cDNA fragments of 300–500 bp are long enough to silence genes in the VIGS system [22]. *N. tabacum* SMO mRNA fragments were inserted into the viral TTO1 vector and used for silencing experiments: the *Nt*SMO1 fragment shares 71–74 % identity with the *At*SMO1 family, and *Nt*SMO2 shares 75 % identity with the *At*SMO2 family and thus falls clearly within these two families. *Nt*SMO1 and *Nt*SMO2 were only 56 % identical with each other and thus were suitable to silence specifically each of the two plant SMO families using the VIGS approach.

*Nt*SMO1 and *Nt*SMO2 cDNA fragments were placed under the control of the tobacco mosaic virus (TMV-U1) coat protein subgenomic promoter in the antisense orientation. Non-infected plants and plants infected with the previously described TTO1A-pepper fruit CCS (capsanthin-capsorubin synthase) construct (TTO1-CCS) [23] were used as controls. Infectious RNAs from TTO1-SMO1 and TTO1-SMO2 were prepared *in vitro* using SP6 DNA-dependent RNA polymerase and used for mechanically inoculating *N. benthamiana*. The viral symptoms consisted of the systemic distortion of leaves, plant stunting and mild chlorosis. In controls infected with TTO1-CCS, additional development of orange patches as described previously [23] attested the efficiency of the infection procedure. In plants infected with TTO1-SMO1 and TTO1-SMO2, we observed no additional phenotype characteristics (results not shown).

The genetic inhibition of the plant SMOs should result in the accumulation of the substrates of the targeted enzymes. Thus, approx. 3 weeks after infection, the sterols of plant series infected either with TTO1-SMO1 or TTO1-SMO2 were analysed. Control plants included non-infected wild-type plants and plants infected with TTO1-CCS. Sterol extracts from young growing stems were quantified by GC and unequivocally identified by coincidental retention time and an electron impact mass spectrum identical with that of authentic standards (Table 1) [19]. Results are shown in Scheme 2, Figure 3 and Table 2.

Table 1 GC-MS (70 eV) analysis of sterols found in wild-type and infected *N. benthamiana*

Compound	TLC: R_f (methylene chloride) (3βOH)	GC: DB1 (3βOH) t_R	Molecular and prominent fragments ions
4,4-Dimethylsterols			
Cycloartenol (D1)	0.44	1.274	M^+ = 468 (17)*, 453 (15), 408 (85), 393 (100), 365 (45), 339 (25), **286 (45)**† , 255 (10)
24-Methylenecycloartenol (D2) (acetate)	0.44	1.340	M^+ = 482 (12), 467 (16), 422 (100), 407 (90), 379 (50), **300 (30)**, 269 (15)
Cycloartanol (D3) (acetate)	0.44	1.234	M^+ = 470 (10), 455 (12), 410 (78), 395 (100), 367 (55), 341 (37), **288 (62)**, 255 (25)
β-Amyrine (Z) (acetate)	0.44	1.222	M^+ = 468 (4), 453 (2), 393 (2), **218 (100)**, 203 (45)
Taraxerol (Y) (acetate)	0.44	1.202	M^+ = 468 (15), 453 (10), 393 (5), 344 (45), 329 (25), 269 (22), 218 (16), 204 (100)
4α-Methylsterols			
Lophenol (M4)	0.38	1.115	M^+ = 400 (100), 385 (28), 382 (14), 367 (12), 287 (15), **269 (77)**, 245 (20), 227 (30)
24-Dehydrolophenol (M7)	0.38	1.133	M^+ = 398 (100), 383 (48), 380 (28), **269 (65)**, **267 (90)**, 227 (60)
Obtusifoliol (X)	0.38	1.178	M^+ = 426 (32), **411 (100)**, 393 (26), 383 (15), 327 (24), 245 (59), 233 (30)
24-Methylenelophenol (M1)	0.38	1.219	M^+ = 412 (9), 397 (17), 379 (8), 328 (20), **285 (100),** 269 (14), 241 (10), 227 (16)
24-Methyllophenol (M5)	0.38	1.234	M^+ = 414 (87), 399 (26), 381 (15), 355 (12), 285 (68), **269 (100)**, 227 (45)
24-Ethyllophenol (M6)	0.38	1.333	M^+ = 428 (100), 413 (30), 395 (9), 287 (21), 285 (21), **269 (90)**, 227 (30)
24-Ethylidenelophenol (M2)	0.38	1.345	M^+ = 426 (2), 411 (4), 393 (2), 328 (31), **285 (100)**, 227 (8)
4-Desmethylsterols			
Cholesterol (S4)	0.27	1.000	M^+ = 386 (100), 368 (59), 353 (43), 301 (56), 275 (69), 255 (32), 247 (19), 231 (21), 213 (40)
Campesterol (S1)	0.27	1.120	M^+ = 400 (100), 382 (67), 367 (47), 315 (61), 289 (64), 273 (37), 255 (47), 231 (26), 213 (63)
Stigmasterol (S2)	0.27	1.162	M^+ = 412 (100), 397 (10), 394 (15), 379 (15), 369 (15), 351 (30), 314 (13), 300 (47), 285 (11), 271 (72), 255 (83), 229 (15), 213 (35)
Sitosterol (S3)	0.27	1.223	M^+ = 414 (100), 396 (48), 381 (34), 329 (53), 303 (48), 273 (27), 255 (32), 231 (21), 213 (37)
Isofucosterol (W)	0.27	1.228	M^+ = 412 (6), 397 (2), 379 (2), 314 (100), 299 (25), 281 (35), 229 (25), 213 (12)

* Percentage relative abundance is given in parentheses.
† Characteristic fragments are shown in boldface.

Since *At*SMO2-1 and *At*SMO2-2 can restore endogenous ergosterol synthesis in *erg25*, we first examined the sterol profile of plants infected with TTO1-SMO2. Results indicate that the quantitative and qualitative sterol profiles of TTO1-SMO2-infected stems were profoundly altered. The most noteworthy difference appeared in the contents of 4α-methylsterols: 24-ethylidenelophenol (M2) and lophenol (M4) accumulated 10–15-fold higher levels when compared with the control plants (Scheme 2, Figure 3 and Table 2). Moreover, 24-ethyllophenol (M6), which was not detected in control series, became a major 4α-methylsterol in TTO1-SMO2 stems. This accumulation of 4α-methyl-Δ^7-sterols led to a 6–7-fold relative increase in the total amount of 4α-methylsterols. In contrast, the 4,4-dimethylsterol profile was not significantly affected. Concerning the desmethylsterol profile (Scheme 2 and Figure 3), including campesterol (S1), sitosterol (S3), stigmasterol (S2) and isofucosterol (W), we observed a substantial lowering of the amount of campesterol (S1), resulting in an increase in the ratio of C-10/C-9 side-chain sterols from 2.1 to 2.3 in wild-type and other series of infected plants and to 3.7 in TTO1-SMO2-infected plants.

Infection with TTO1-SMO1 also affected the sterol profile of *N. benthamiana* stems. In this case, the most noteworthy difference was observed in the contents of 4,4-dimethylsterols. Importantly, a marked increase in the 24-methylenecycloartanol (D2) level (Scheme 2, Figure 3 and Table 2) was seen, which was 4–6-fold higher compared with that found in different series of control plants and plants infected with TTO1-SMO2. In addition, a significant average 2–4-fold accumulation of cycloartenol (D1) and cycloartanol (D3) was also observed in the stems infected with TTO1-SMO1. This accumulation of 4,4-dimethyl-9β,19-cyclopropylsterols led to a 3-fold relative increase in the total level of 4,4-dimethylsterols when compared with the different series of control and TTO1-SMO2 plants. In contrast, the 4α-methylsterol and desmethylsterol profiles of the TTO1-SMO1 plants remained unchanged (Scheme 2, Figure 5 and Table 2).

Transcript levels of *N. benthamiana* SMO genes

To examine the effects of VIGS on the endogenous amounts of mRNA for the *Nb*SMO1 and *Nb*SMO2 genes, the transcript levels were estimated by semi-quantitative RT–PCR on a RNA total extract, as described in the Materials and methods section, using mRNA encoding *N. benthamiana* actin as an internal standard. *Nb*SMO1 and *Nb*SMO2 were only 51 % identical with each other and thus were suitable for quantifying specifically the transcript amounts of each of the two endogenous *Nb*SMO cDNA families.

As shown in Figure 4, an average 3-fold reduction in RT–PCR products amplified with *Nb*SMO1 primers was observed in SMO1-silenced plants, with negligible change in the level of SMO2 transcripts. Conversely, the results in Figure 4 indicate also a reduction in RT–PCR products amplified with *Nb*SMO2 primers in SMO2-silenced plants, with minor effects on the level of SMO1 transcripts. In addition, the amounts of *Nb*SMO1 and *Nb*SMO2 transcripts of wild-type plants were similar under our experimental conditions (results not shown). These results confirmed efficiency and specificity of silencing of SMO1 or SMO2 genes in *N. benthamiana*.

Taken together, the substantial and specific accumulation of 4,4-dimethyl-9β,19-cyclopropylsterols or 4α-methyl-Δ^7-sterols in TTO1-*Nt*SMO1- or TTO1-*Nt*SMO2-infected plants was consistent with a corresponding deficiency of SMO1 and SMO2 transcripts.

DISCUSSION

The plant SMO cDNAs that we have cloned in the present study were found to fall into two families, SMO1 and SMO2. The clearly distinct organization of coding domains between both the families would suggest their early divergence. Analysis of the deduced amino acid sequences revealed in every case the presence of three histidine-rich motifs that exhibit a topology and spacing of amino acids characteristic of the *ERG3–ERG25*

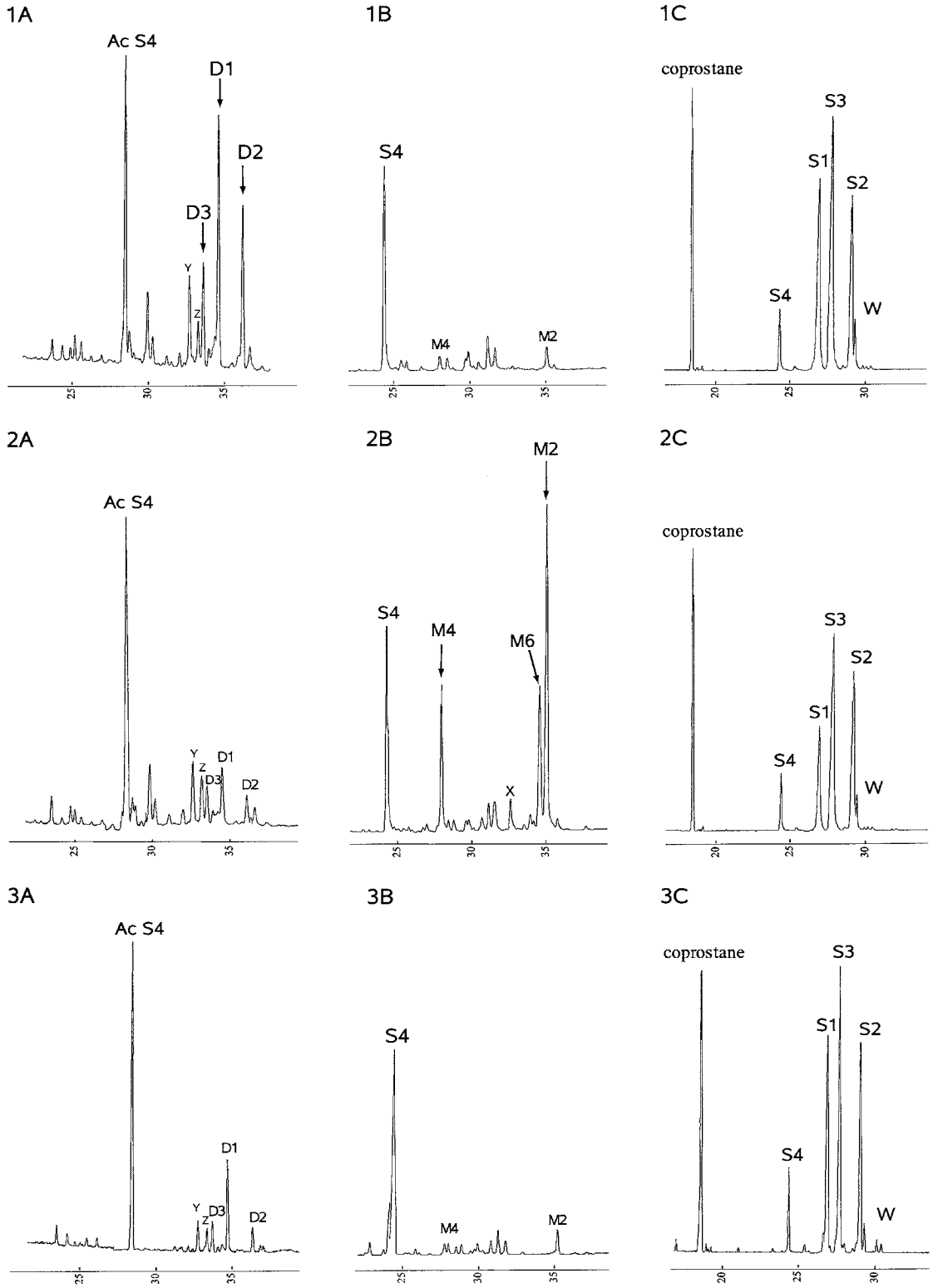

Figure 3 GC profiles of sterols of non-infected *N. benthamiana* and *N. benthamiana* infected with TTO1-SMO1 or TTO1-SMO2

Numbers refer to: 1, SMO1-infected plant; 2, SMO2-infected plant; 3, non-infected control plant. Letters refer to different sterol fractions: (**A**) 4,4-dimethylsterols (analysed as their acetate derivatives), (**B**) 4α-methylsterols and (**C**) 4-desmethylsterols. GC-MS analysis indicates the accumulation of 24-methylenecycloartanol (D2), cycloartenol (D1) and cycloartanol (D3), induced by infection with viral RNA of TTO1-SMO1 in *N. benthamiana* (**1A**) in comparison to infection with viral RNA of TTO1-SMO2 fragment (**2A**) and to non-infected control plant (**3A**). Z, β-amyrine; Y, taraxerol. Conversely, GC-MS analysis indicates the accumulation of 24-ethylidenelophenol (M2), 24-ethyllophenol (M6) and lophenol (M4), induced by infection with TTO1 vector expressing an SMO2 fragment in *N. benthamiana* (2B) in comparison to infection with TTO1 vector expressing an SMO1 fragment (1B) and to non-infected control plant (3B). The amount of dry material analysed was similar (300 ± 10 mg) for the three representative plants 1, 2 and 3. The amounts of standards, cholesterol (S4) and coprostane were identical in each of the 4,4-dimethylsterol, 4α-methylsterol and 4-desmethylsterol fractions respectively.

Table 2 Sterol composition of young growing stems of non-infected *N. benthamiana* and *N. benthamiana* inoculated with different TTO1 viral transcripts

Results are expressed as a percentage of total sterols.

	Non-infected	TTO1-CCS	TTO1-*Nt*SMO1	TTO1-*Nt*SMO2
No. of plants analysed separately	3	3	6	4
4,4-Dimethylsterols				
Cycloartenol (D1)	1.2 ± 0.2	0.7 ± 0.1	**1.9*** ± 0.8	1.1 ± 0.3
Cycloartanol (D3)	0.7 ± 0.2	0.4 ± 0.1	**1.0** ± 0.4	0.4 ± 0.1
24-Methylenecycloartanol (D2)	0.4 ± 0.05	0.4 ± 0.05	**1.7** ± 0.5	0.4 ± 0.1
Total	2.0 ± 0.2	1.4 ± 0.1	**4.5** ± 1.5	1.9 ± 0.4
4α-Methylsterols				
Obtusifoliol (X)	0.3 ± 0.1	0.3 ± 0.05	0.3 ± 0.05	0.3 ± 0.05
Lophenol (M4)	0.2 ± 0.05	0.2 ± 0.05	0.3 ± 0.1	**2.4** ± 0.8
24-Dehydrolophenol (M7)	0.1 ± 0.1	0.1 ± 0.1	0.1 ± 0.1	0.4 ± 0.2
24-Methylenelophenol (M1)	0.6 ± 0.1	0.7 ± 0.1	0.7 ± 0.2	0.9 ± 0.1
24-Methyllophenol (M5)	0.3 ± 0.05	0.6 ± 0.1	0.5 ± 0.1	0.9 ± 0.1
24-Ethylidenelophenol (M2)	0.6 ± 0.1	0.6 ± 0.1	0.7 ± 0.1	**5.9** ± 1.9
24-Ethyllophenol (M6)	n.d.	n.d.	0.1 ± 0.1	**2.0** ± 1.2
Total	1.8 ± 0.1	2.1 ± 0.1	2.4 ± 0.4	**12.3** ± 3.9
Desmethylsterols				
Cholesterol (S4)	6.3 ± 1.2	5.6 ± 0.3	5.2 ± 0.7	5.7 ± 1.2
Campesterol (S1)	28 ± 0.4	28 ± 2	27 ± 1	18 ± 2
Sitosterol (S3)	23 ± 1	26 ± 2	21 ± 1	25 ± 2
Stigmasterol (S2)	35 ± 1	33 ± 1	36 ± 2	33 ± 2
Isofucosterol (W)	3.6 ± 0.7	4 ± 0.7	4 ± 0.7	4 ± 1.4
Total	96 ± 1	96 ± 0.5	92 ± 1	85 ± 4
Total sterols (μg/g)	267 ± 60	200 ± 40	326 ± 84	215 ± 60

* Values that have increased after infection are shown in boldface.

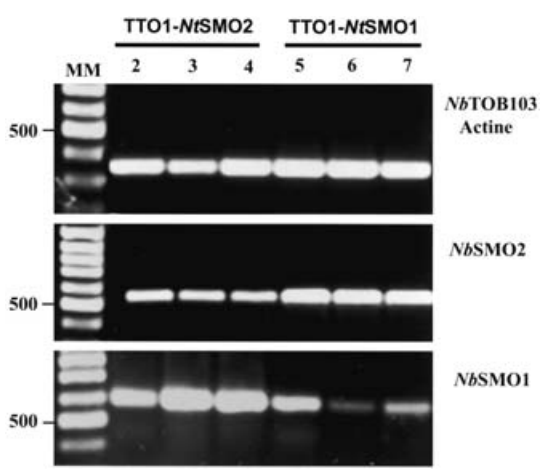

Figure 4 Effects of VIGS on the transcription of *Nb*SMO genes

RT–PCR analysis showed the effects of VIGS on the transcription of *Nb*SMO1 and *Nb*SMO2. The ethidium bromide-stained agarose gels show RT–PCR products. Molecular-mass standards (MM) are shown in the first lane and the gels show the 333, 520 and 595 bp bands for PCR products of actin, *Nb*SMO2 and *Nb*SMO1 respectively. Lanes 2–4 correspond to products from three distinct TTO1-*Nt*SMO2-infected plants and lanes 5–7 to products from three distinct TTO1-*Nt*SMO1-infected plants. The PCR products were routinely excised from the gel, and their identities were confirmed by nucleotide sequence analysis to be 100 % identical with the actin, *Nb*SMO1 and *Nb*SMO2 fragments respectively.

family (PFAM01598; Figure 1). This family includes integral membrane enzymes catalysing desaturations and hydroxylations: AtSMO1 and AtSMO2 proteins show 18–20 and 18–19 % identity respectively with the recently characterized *A. thaliana* SUR2 (C-4-sphingolipid hydroxylase) gene [24] and only 14–18 and 20 % identity with the *A. thaliana* Δ^7-sterol-C-5(6)-desaturase (ERG3) [25,26]. Moreover, the spacing and topology of the histidine motifs are clearly distinct from those found in the extended family of membrane-bound fatty acid desaturases/hydroxylases [27]. One possible function for these tripartite motifs would be to provide the ligands for a presumed catalytic di-iron centre, as proposed previously for other enzymes possessing these motifs and catalysing desaturations or hydroxylations [27,28]. Incidentally, we have demonstrated recently, by mutational analysis of the recombinant *A. thaliana* Δ^7-sterol-C5(6)-desaturase (ERG3), that all the eight individual histidine residues were essential for catalysis by this oxygenase [26].

Interestingly, the central conserved domain of the two plant SMO families and the yeast SMO, including the above histidine-rich motifs, contrasted with the poor homology of the N-terminal domains. These local N-terminal divergences could be correlated with the clearly distinct plant and yeast SMO substrate specificities and/or interactions with other components of the demethylation complex. Particularly, for SMO1, the higher divergence of the N-terminal domain could be linked to the recognition of the particular structure of 9β,19-cyclopropylsterols specific to plants. Furthermore, we took advantage of these least-conserved regions in the design of the cDNA fragments used in the VIGS experiments. Indeed, PCR primers were designed so that the PCR-produced fragments would start immediately on the 3′-side of the first of the three histidine-rich motifs found in all SMOs, whereas the 5′-primers were positioned in such a way to include the maximum length of the least-conserved N-terminal domain of the SMOs.

Heterologous expression in yeast and functional complementation of yeast mutants have been shown previously to be powerful tools to characterize genes of the plant sterol pathway [29]. For SMO, one mutant was available, namely *erg25-25c*, which lacks sterol C-4-methyl oxidation activity [13]. Complementation of this mutant by plant SMO cDNAs inserted into a vector optimized for yeast expression was expected to restore both growth in the absence of ergosterol and endogenous ergosterol biosynthesis. Two groups of complementation were obtained with plant SMO cDNAs: the SMO2 group of complementation restored growth, but restored only low levels of ergosterol biosynthesis. The SMO1 group did not complement *erg25-25c*. These results suggest that only one family of SMOs is functional for the oxidation of 4,4-dimethylzymosterol (V), the substrate of the yeast SMO accumulating in *erg25*. It could reflect a strict and distinct substrate specificity of the SMO1 isoenzymes unable to oxidize 4,4-dimethylzymosterol (V) in contrast with the *S. cerevisiae* SMO and the SMO2 isoenzymes.

To characterize precisely the function of each of the two plant SMO families, we used a VIGS approach and searched for clear and distinct biochemical phenotypes, consisting of specific accumulation of substrates of targeted SMOs, after infection of young *N. benthamiana* plants with a viral RNA containing cDNA fragments corresponding to each family of SMOs. VIGS has been suggested to be an efficient method to suppress the endogene function of a target gene by expressing a partial sequence of this gene from a virus-based vector [15,22,30,31]. This approach allows different levels of silencing and this is particularly useful for partially down-regulating potentially lethal genes. Owing to the possible lethality of the SMO genes in plants, a weak phenotype was more interesting than a complete silencing of plant SMOs. In addition, in the case of gene redundancy as in *Arabidopsis* or *Nicotiana*, VIGS can be used to reveal the collective function of the isoform family in the trait of interest. In our case, similar to previous reports, RNA silencing in both monocot

and dicot plants is efficient only with sequences that are 88–100% identical with the endogenous gene target [15,22]. To ensure sufficient identity to be able to silence the expression of *N. benthamiana* SMO genes, we inserted *Nicotiana* SMO gene fragments into the TTO1 viral vector, which has been previously used to manipulate the carotenoid biosynthetic pathway in *N. benthamiana* [15].

The VIGS experiments performed in the present study led to young *N. benthamiana* plants exhibiting clear and distinct biochemical phenotypes. Remarkably, on one hand, SMO1-silenced plants displayed a specific increase in the level of 4,4-dimethyl-9β,19-cyclopropylsterols and conserved qualitative and quantitative standard levels of 4α-methylsterols; on the other, SMO2-silenced plants displayed a specific increase in the level of 4α-methyl-Δ^7-sterols and conserved qualitative and quantitative standard levels of 4,4-dimethylsterols. Moreover, since these respective biochemical phenotypes are observed in several distinct infected plants, but not in plants infected with TTO-CCS or non-infected plants, they can confidently be ascribed to the presence of the *Nt*SMO1 and *Nt*SMO2 cDNAs. These clear and distinct biochemical changes obtained after infection with TTO1-SMO1 and TTO1-SMO2, which correlate well with the specific decreases in the *Nb*SMO1 and *Nb*SMO2 mRNA levels respectively, confirm the genetic silencing of the corresponding SMO endogenes.

Silencing of SMO2 in *N. benthamiana* resulted in a major accumulation of 24-ethylidenelophenol (M2) and its reduced derivative 24-ethyllophenol (M6; Scheme 2). The high accumulation of 4α-methyl-Δ^7-sterols possessing a C-24-ethylidene or ethyl substituent probably reflects the subsequent rapid methylation of transiently accumulated 24-methylenelophenol (M1) to produce (M2) by SMT2 [sterol methyltransferase 2 = SAM (*S*-adenosyl-L-methionine)-24-methylenelophenol C-24^1-methyltransferase], consistent with the substrate preference of this enzyme [32,33]. Furthermore, the increased C-24-ethyl/C-24-methyl side-chain ratio (3.7) of desmethylsterols in SMO2-silenced plants correlated well with the accumulation of such 4α-methylsterol, 24-ethylsterol or ethylidene-Δ^7-sterol precursors. Incidentally, this could suggest that down-regulation or overexpression of SMO2 could indirectly modulate the ethyl/methyl end-product sterol ratio (sitosterol/campesterol) and interfere with phases of plant development or growth depending on this ratio [34].

Taken together, the obtained sterol profiles indicate that 4,4-dimethyl-9β,19-cyclopropylsterols such as D2 and D3 were the preferred substrates of SMO1 and 4α-methyl-Δ^7-sterols such as M1 and M2 the preferred substrates of SMO2. These specific accumulations of 4,4-dimethylsterols or 4α-methylsterols are consistent with a poor overlapping in the substrate specificities of these two families of tobacco SMOs, leading to the clearly distinct biochemical phenotypes observed in the present study. These results compared remarkably well with the clearly distinct substrate specificities previously determined for the native microsomal maize SMOs [10].

Recent studies in *A. thaliana* indicate that the plants compromised early in the sterol biosynthetic pathway, i.e. upstream of the *fackel* mutant defective in C-14-reductase (Schemes 1 and 2) [7,8], show severe defects in development and embryogenesis, whereas those affected later in the pathway, such as *dwf7*/*ste1* [35] or *dwf1*/*DIM* [36], do not. Thus, in the event of an impaired expression of the biosynthetic genes upstream of the sterol C-14-reduction step, plants might develop regulation processes to decrease these defects. In the present study, induction of such a process could be reflected by the smaller biochemical changes observed in SMO1 when compared with SMO2-silenced tissues situated upstream or downstream of sterol 14-reductase (Scheme 2), under identical experimental conditions. As a possible effect of such a regulation process, the total amount of sterols in SMO1-silenced tobacco (326 μg/g) was significantly higher compared with that in other series, including SMO2-silenced plants (200–270 μg/g).

To summarize, results of the present study clearly ascribe the function of SMO1 as a 4,4-dimethyl-9β,19-cyclopropylsterol-4α-methyl oxidase and SMO2 as a 4α-methyl-Δ^7-sterol-4α-methyl oxidase, thereby indicating that in photosynthetic eukaryotes, two distinct families of sterol C-4-methyl oxidases control the level of 4,4-dimethylsterol and 4α-methylsterol precursors respectively. Thus sterol biosynthesis in plants is markedly different from that found in animals and fungi, where a single C-4-methyl oxidase gene is involved in the removal of both methyl groups at C-4 (Scheme 1). To our knowledge, plant mutants affected by SMO activity have not been reported so far. In this respect, the present study could give important clues for the elucidation of the physiological roles of 4,4-dimethylsterol and 4α-methylsterol and of the biological significance of the existence of two distinct C-4-demethylation complexes in photosynthetic eukaryotes. Finally, the present identification of two gene families in higher plants, which encode SMO possessing distinct substrate specificities, will allow a structure–function study of the protein domains controlling this specificity.

We are indebted to A. Hoeft (IBMP, Strasbourg, France) for GC and GC-MS analyses and helpful technical assistance. We thank Biosource Technologies (Vacaville, CA, U.S.A.) for providing the TTO1 vector. We are grateful to Dr M. Bard (Indiana University, Indianapolis, IN, U.S.A.) for providing the yeast mutant *erg25-25c*. We thank Dr M. Taton and Dr G. Vetter (IBMP) for their participation in the preliminary phase of this work. We are indebted to Dr M. A. Hartmann (IBMP) and Dr J. D. Faure (INRA, Laboratoire de Biologie Cellulaire, Versailles, France) for a critical reading of the manuscript and to Professor B. Camara (IBMP) for helpful discussions.

REFERENCES

1 Bloch, K. E. (1983) Sterol structure and membrane function. CRC Crit. Rev. Biochem. **14**, 47–92
2 Hartmann, M. A. (1998) Plant sterols and the membrane environment. Trends Plant Sci. **2**, 137–143
3 Clouse, S. D. (2002) *Arabidopsis* mutants reveal multiple roles for sterols in plant development. Plant Cell **14**, 1995–2000
4 Bishop, G. J. and Yokota, T. (2001) Plants steroid hormones, brassinosteroids: current highlights of molecular aspects on their synthesis/metabolism, transport, perception and response. Plant Cell Physiol. **42**, 114–120
5 Benveniste, P. (1986) Sterol biosynthesis. Annu. Rev. Plant Physiol. **37**, 275–308
6 Benveniste, P. and Rahier, A. (1992) Target sites of sterol biosynthesis inhibitors in plants. In Target Sites of Fungicide Action (Köller, W., ed.), pp. 207–225, CRC Press, Boca Raton, FL
7 Schrick, K., Mayer, U., Horrichs, A., Kuhnt, C., Bellini, C., Dangl, J., Schmidt, J. and Jurgens, G. (2000) FACKEL is a sterol C-14 reductase required for organized cell division and expansion in *Arabidopsis* embryogenesis. Genes Dev. **14**, 1471–1484
8 Jang, J.-C., Fujioka, S., Tasaka, M., Seto, H., Takatsuto, S., Ishii, A., Aida, M., Yoshida, S. and Sheen, J. (2000) A critical role of sterols in embryonic patterning and meristem programming revealed by the *fackel* mutants of *Arabidopsis thaliana*. Genes Dev. **14**, 1485–1497
9 Schrick, K., Mayer, U., Martin, G., Bellini, C., Kuhnt, C., Schmidt, J. and Jürgens, G. (2002) Interactions between sterol biosynthesis genes in embryonic development of *Arabidopsis*. Plant J. **31**, 61–73
10 Pascal, S., Taton, M. and Rahier, A. (1993) Plant sterol biosynthesis: identification and characterization of two distinct microsomal oxidative enzymatic systems involved in sterol C4-demethylation. J. Biol. Chem. **268**, 11639–11654
11 Rondet, S., Taton, M. and Rahier, A. (1999) Identification, characterization, and partial purification of 4α-carboxysterol-C3-dehydrogenase/C4-decarboxylase from *Zea mays*. Arch. Biochem. Biophys. **366**, 249–260
12 Pascal, S., Taton, M. and Rahier, A. (1994) Plant sterol biosynthesis: identification of a NADPH dependent sterone reductase involved in sterol-4 demethylation. Arch. Biochem. Biophys. **312**, 260–271

13 Bard, M., Bruner, P. A., Pierson, C. A., Lees, N. D., Biermann, B., Frye, L., Koegel, C. and Barbuch, R. (1996) Cloning and characterization of *ERG25*, the *Saccharomyces cerevisiae* gene encoding C-4 sterol methyl oxidase. Proc. Natl. Acad. Sci. U.S.A. **93**, 186–190
14 Vernet, T., Dignard, D. and Thomas, D. Y. (1987) A family of yeast expression vectors containing the phage f1 intergenic region. Gene **52**, 225–233
15 Kumagai, M. H., Donson, J., Della-Cioppa, G., Harvey, D., Hanley, K. and Grill, L. K. (1995) Cytoplasmic inhibition of carotenoid biosynthesis with virus-derived RNA. Proc. Natl. Acad. Sci. U.S.A. **92**, 1679–1683
16 Darnet, S., Bard, M. and Rahier, A. (2001) Functional identification of sterol-4α-methyl oxidase cDNAs from *Arabidopsis thaliana* by complementation of a yeast *erg25* mutant lacking sterol-4α-methyl oxidation. FEBS Lett. **508**, 39–43
17 Moniz de Sa, M. and Drouin, G. (1996) Phylogeny and substitution rates of angiosperm actin genes. Mol. Biol. Evol. **13**, 1198–1212
18 Gietz, D., St Jean, A., Woods, R. A. and Schiestl, R. H. (1992) Improved method for high efficiency transformation of intact yeast cells. Nucleic Acids Res. **20**, 1425–1432
19 Rahier, A. and Benveniste, P. (1989) Mass spectral identification of phytosterols. In Analysis of sterols and other significant steroids (Nes, W. D. and Parish, E., eds.), pp. 223–250, Academic Press, New York
20 Hanley, B. A. and Schuler, M. A. (1988) Plant intron sequences: evidence for distinct groups of introns. Nucleic Acids Res. **16**, 7159–7176
21 Darnet, S. and Rahier, A. (2003) Enzymological properties of sterol-C-4-methyl-oxidase of yeast sterol biosynthesis. Biochim. Biophys. Acta **1633**, 106–117
22 Ruiz, M. T., Voinet, O. and Baulcombe, D. C. (1998) Initiation and maintenance of virus-induced gene silencing. Plant Cell **10**, 937–946
23 Kumagai, M. H., Keller, Y., Bouvier, F., Claty, D. and Camara, B. (1998) Functional integration of non-native carotenoids into chloroplasts by viral-derived expression of capsanthin-capsorubin synthase in *Nicotiana benthamiana*. Plant J. **14**, 305–315
24 Sperling, P., Ternes, P., Moll, H., Franke, S., Zähringer, U. and Heinz, E. (2001) Functional characterization of sphingolipid C4-hydroxylase genes from *Arabidopsis thaliana*. FEBS Lett. **494**, 90–94
25 Gachotte, D., Hüsselstein, T., Bard, M., Lacroute, F. and Benveniste, P. (1996) Isolation and characterization of an *Arabidopsis thaliana* cDNA encoding a Δ^7-sterol-C-5-desaturase by functional complementation of a defective yeast mutant. Plant J. **9**, 391–398
26 Taton, M., Husselstein, T., Benveniste, P. and Rahier, A. (2000) Role of high conserved residues in the reaction catalyzed by recombinant Δ^7-sterol-C(5)6-desaturase studied by site-directed mutagenesis. Biochemistry **39**, 701–711
27 Shanklin, J. and Cahoon, E. B. (1998) Desaturation and related modifications of fatty acids. Annu. Rev. Plant Physiol. Plant Mol. Biol. **49**, 611–641
28 Lee, M., Leumann, M., Banas, A., Bafor, M., Singh, S., Schweizer, M., Nilsson, R., Liljarberg, C., Dahlqvist, A., Gummeson, P. O. et al. (1998) Identification of non-heme diiron proteins that catalyze triple bond and epoxy group formation. Science **280**, 915–918
29 Bach, T. J. and Benveniste, P. (1997) Cloning of cDNAs or genes encoding enzymes of sterol biosynthesis from plants and other eukaryotes: heterologous expression and complementation analysis of mutations for functional characterization. Prog. Lipid Res. **36**, 197–226
30 Baulcombe, D. C. (1999) Fast forward genetics based on virus-induced gene silencing. Curr. Opin. Plant Biol. **2**, 109–113
31 Wang, M. and Waterhouse, P. M. (2001) Application of gene silencing in plants. Curr. Opin. Plant Biol. **5**, 146–150
32 Rahier, A., Taton, M., Bouvier-Navé, P., Schmitt, P., Benveniste, P., Schuber, A. S., Narula, A. S., Cattel, L., Anding, C. and Place, P. (1986) Design of high energy intermediate analogues to study sterol biosynthesis in higher plants. Lipids **21**, 52–62
33 Rahier, A., Génot, J. C., Schuber, F., Benveniste, P. and Narula, A. S. (1984) Inhibition of *S*-adenosyl-L-methionine sterol C24 methyl transferase by analogues of a carbocationic ion high energy intermediate. J. Biol. Chem. **259**, 15215–15223
34 Schaeffer, A., Bronner, R., Benveniste, P. and Schaller, H. (2001) The ratio of campesterol to sitosterol that modulates growth in *Arabidopsis* is controlled by sterol methyltransferase 2;1. Plant J. **25**, 605–615
35 Choe, S., Noguchi, T., Fijioka, S., Takatsuto, S., Tissier, C., Gregory, B., Ross, A., Tanaka, A., Yoshida, S., Tax, F. E. et al. (1999) The *Arabidopsis dwf7/ste1* mutant is defective in the Δ^7 sterol C-5 desaturation step leading to brassinosteroid biosynthesis. Plant Cell **11**, 207–221
36 Choe, S., Dilkes, B. P., Gregory, B. D., Ross, A. S., Yuan, H., Noguchi, T., Fujioka, S., Takatsuto, S., Tanaka, A., Yoshida, S. et al. (1999) The *Arabidopsis* dwarf1 mutant is defective in the conversion of 24-methylenecholesterol to campesterol in brassinosteroid biosynthesis. Plant Physiol. **119**, 897–907

Received 14 October 2003/17 November 2003; accepted 4 December 2003
Published as BJ Immediate Publication 4 December 2003, DOI 10.1042/BJ20031572